



Molybdenum Disulfide (MoS₂) Nanoflakes as Inherently Electroactive Labels for DNA Hybridization Detection

Journal:	<i>Nanoscale</i>
Manuscript ID:	NR-ART-07-2014-003795.R1
Article Type:	Paper
Date Submitted by the Author:	29-Jul-2014
Complete List of Authors:	Loo, Adeline; Nanyang Technological University, Chemistry and Biological Chemistry Bonanni, Alessandra; Nanyang Technological University, Chemistry and Biological Chemistry Ambrosi, Adriano; Nanyang Technological University, Chemistry and Biological Chemistry Pumera, Martin; Nanyang Technological University, Chemistry and Biological Chemistry

Cite this: DOI: 10.1039/c0xx00000x

www.rsc.org/xxxxxx

ARTICLE TYPE

Molybdenum Disulfide (MoS₂) Nanoflakes as Inherently Electroactive Labels for DNA Hybridization Detection

Adeline Huiling Loo, Alessandra Bonanni,* Adriano Ambrosi and Martin Pumera*

Received (in XXX, XXX) Xth XXXXXXXXX 20XX, Accepted Xth XXXXXXXXX 20XX

DOI: 10.1039/b000000x

The detection of specific DNA sequences plays a critical role in the areas of medical diagnostics, environmental monitoring, drug discovery and food safety. This has therefore become a strong driving force behind the ever-increasing demand for simple, cost-effective, highly sensitive and selective DNA biosensors. In this study, we report for the first time, a novel approach for the utilization of molybdenum disulfide nanoflakes, a member of the transition metal dichalcogenides family, in the detection of DNA hybridization. Herein, molybdenum disulfide nanoflakes serve as inherently electroactive labels, with the inherent oxidation peak exploited as the analytical signal. The principle of detection is based on the differential affinity of molybdenum disulfide nanoflakes towards single-stranded DNA and double-stranded DNA. The employment of transition metal dichalcogenides nanomaterials for sensing and biosensing purposes represents an upcoming research area which holds great promise. Hence, our findings are anticipated to have significant contributions towards the fabrication of future DNA biosensors.

Introduction

Single-layered transition metal dichalcogenides (TMDs), with a similar two-dimensional (2D) structure as graphene, demonstrate chemical versatility. Hence, single-layered TMDs hold great potential for fundamental and technological research in a wide range of areas consisting of energy storage, catalysis, sensing and electronic devices.¹ Single-layered TMDs is comprised of transition metal atoms surrounded in a sandwich structure by chalcogen atoms which are covalently bonded to the transition metal atoms, whereas the interactions between the individual layers are of van der Waals type. Parallel to graphene, individual layers of TMDs are isolated from their bulk forms through intercalation methods or mechanical cleavage^{2, 3} and exfoliation of these materials into single or few-layers generally leads to additional characteristics as a result of confinement effects.⁴⁻⁶ Hence, it is with high expectations that the chemistry of TMDs materials presents prospects for uncovering new research directions for inorganic 2D materials.¹

As one of the more studied TMDs, molybdenum disulfide (MoS₂) nanosheet has garnered considerable attention from researchers due to its large surface specific area and its excellent optical, mechanical, and electronic properties.⁷⁻¹² From a structural point of view, MoS₂ nanosheet is constituted of three atomic layers: one Mo metal layer sandwiched between two S layers by covalent bonds. Such three-layer stacks are then held together by weak van der Waals interactions.¹³ As a result of this layered structure, MoS₂ presents interesting electronic properties which are different perpendicularly to the *c*-axis (along the plane)

from those in perpendicular direction. In addition, significant electrochemical and catalytic differences can be found between basal plane portion of the material and its edges.¹⁴ This is because the 2D electron-electron correlations among Mo atoms would assist in the enhancement of planar electric transportation properties.¹⁵ In view of these exceptional features, MoS₂ nanosheet has been employed in various areas such as sensors,^{16, 17} fuel cells¹⁴ and transistors¹⁸ thus far. In particular, the application of MoS₂ nanosheet in sensing and biosensing devices represents an upcoming research direction.

Till date, there have just been a number of studies performed on the utilization of MoS₂ nanosheet in the research field of sensing and biosensing. In these studies, MoS₂ nanosheet is mainly involved as a fluorescence quencher^{19, 20} or as the transducing platform, either by itself^{17, 21} or in the form of a composite with other components such as nanoparticles^{22, 23} and polymers.^{24, 25} Herein, we report a novel approach of employing MoS₂ nanoflakes as an electroactive label for the voltammetric detection of DNA hybridization, correlating to the diagnosis of Alzheimer's disease. The rationale behind our approach lies in the inherent electroactivity of MoS₂ nanoflakes, originating from the oxidation of the nanoflakes, as well as the differential affinity of the nanoflakes towards single and double-stranded DNA.^{19, 20}

Results and Discussions

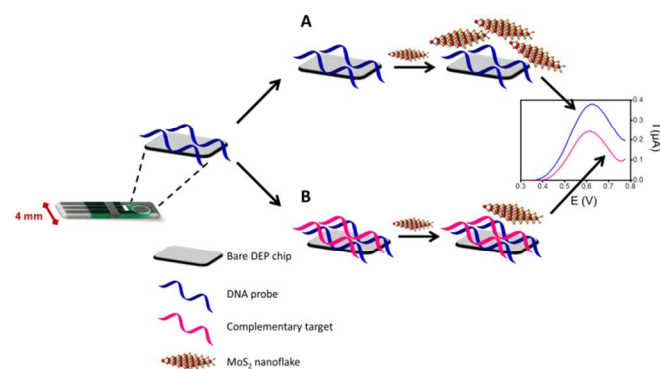
Herein, we investigate the interactions between molybdenum disulfide (MoS₂) nanoflakes and DNA strands for the detection of DNA hybridization, correlating to the diagnosis of Alzheimer's disease. It is demonstrated that MoS₂ nanoflakes have a different

degree of interactions with single-stranded DNA (ssDNA) and double-stranded DNA (dsDNA).¹⁹ Hence, by utilizing the different degree of interactions which MoS₂ nanoflakes exhibit with DNA strands, as well as the electrochemical behavior of MoS₂ nanoflakes, we propose a sensing strategy for DNA hybridization with MoS₂ nanoflakes functioning as electroactive labels.

The electrochemical behaviour of MoS₂ nanoflakes was investigated by performing cyclic voltammetry between 2.0 to -2.0 V. As demonstrated in Figure S1 (Supporting information), a series of oxidation waves were observed in the first scan only. This suggests that the oxidation of MoS₂ nanoflakes is chemically irreversible. Subsequently, the oxidation wave at ~ 0.62 V was employed as the analytical signal for the aim of DNA sensing, as oxidation waves at other potentials faced interferences. In addition, differential pulse voltammetry technique was then adopted over cyclic voltammetry due to improved sensitivity.

Scheme 1 illustrates the sensing strategy employed in this study. First of all, ssDNA probe was immobilized onto the surface of bare disposable electrical printed (DEP) carbon chip via physical adsorption. Upon the addition of complementary DNA target (Path B), the ssDNA probe hybridized with the complementary DNA target to form a dsDNA duplex. Subsequently, the modified DEP chips (Path A and B) were exposed to MoS₂ nanoflakes for conjugation. As demonstrated in Scheme 1, MoS₂ nanoflakes conjugated to the modified DEP chips surfaces to different extent depending on the presence of complementary DNA target. As such, a different amount of MoS₂ nanoflakes was affixed onto the modified DEP chips surfaces and voltammetric signals of varying intensities were attained.

Specifically, for the case of Path A, MoS₂ nanoflakes could effectively adsorb onto the immobilized ssDNA probe via van der Waals forces of attractions between the nucleobases and the basal plane of MoS₂ nanoflakes. In contrast, when the ssDNA probe underwent hybridization with its complementary DNA target (Path B), the nucleobases involved in the formation of the double helix became buried deep within the densely negatively charged helical phosphate backbone, and the degree of interactions between the resulting dsDNA duplex and MoS₂ nanoflakes was severely reduced. Hence, ssDNA has a higher affinity with MoS₂ nanoflakes as compared to dsDNA and a significantly higher amount of MoS₂ nanoflakes was conjugated to the ssDNA probe modified DEP chip surface in relative to dsDNA duplex modified DEP chip surface and thus, a greater voltammetric signal, stemming from the oxidation of MoS₂ nanoflakes, was achieved for the former case.



Scheme 1. Schematic illustration of the experimental approach adopted.

In order to validate that MoS₂ nanoflakes indeed have a different degree of interactions with ssDNA and dsDNA, DNA hybridization experiments were conducted with three different DNA sequences (complementary, single-base mismatch and non-complementary targets) with the attained results displayed in Figure 1.

In detail, when the hybridization experiment was conducted using the complementary sequence, a comparatively lowest oxidation voltammetric signal was produced (black line). For the instance of single-base mismatch sequence, a higher voltammetric signal was achieved (red line) and finally for the instance of non-complementary sequence, the highest voltammetric signal was obtained (blue line). This signifies that the smallest amount of MoS₂ nanoflakes was conjugated to the modified DEP chip surface when hybridization was performed with complementary sequence, followed by single-base mismatch sequence and lastly non-complementary sequence.

The observed trend could be attributed to the different degree of hybridization efficiency demonstrated by the three sequences. Explicitly, the complementary sequence demonstrated the highest hybridization efficiency and the modified DEP chip surface consisted mainly of dsDNA strands upon the hybridization step. In contrast, for the case of non-complementary sequence, the modified DEP chip surface consisted primarily of non-hybridized ssDNA probe strands due to its poor hybridization efficiency. As described earlier, ssDNA possesses higher affinity with MoS₂ nanoflakes as compared to dsDNA, hence, the highest amount of MoS₂ nanoflakes would be affixed onto modified DEP chip which had undergone incubation with non-complementary sequence. Conversely, for the instance of complementary sequence, the amount of conjugated MoS₂ nanoflakes would be the lowest. Therefore, the largest voltammetric signal was displayed after incubation with non-complementary sequence. In the case of single-base mismatch sequence, its voltammetric signal was greater than the complementary sequence due to the occurrence of partial hybridization. Hence, through these control experiments, it was validated that MoS₂ nanoflakes have a different extent of interactions with ssDNA and dsDNA, with ssDNA having a higher affinity for the nanoflakes than dsDNA, and the intensity of the voltammetric signal reflects the amount of MoS₂ nanoflakes which were conjugated to the modified DEP chips surfaces.

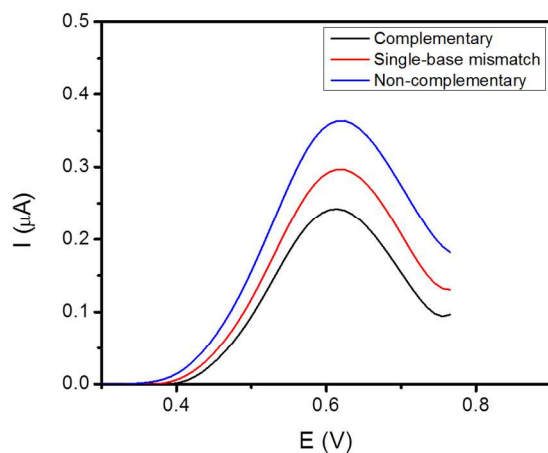


Figure 1. Differential pulse voltammograms of the MoS₂ nanoflakes oxidation peak when the hybridization step was performed with complementary sequence (black), single-base mismatch sequence (red) and non-complementary sequence (blue). The concentration of DNA probe, DNA targets and MoS₂ nanoflakes employed was 10 μM, 300 nM and 0.018 mg/mL respectively. All electrochemical measurements were conducted in 0.1 M PBS buffer solution (pH 7.0) under ambient conditions.

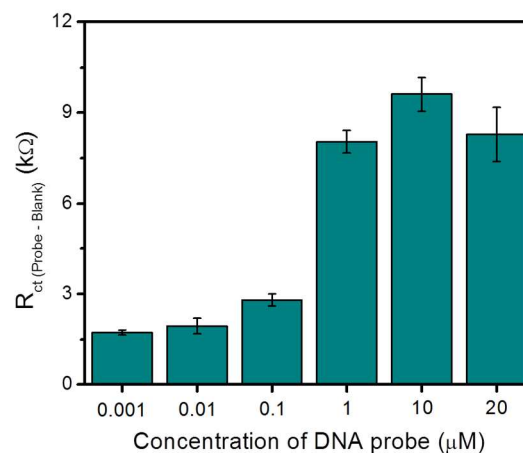


Figure 2. Impedimetric response towards different concentration of DNA probe deposited on the surface of bare DEP chip. Signal is displayed as $R_{ct}(\text{Probe} - \text{Blank})$. Error bars correspond to the standard deviations obtained from triplicate experiments. All electrochemical measurements were performed with 10 mM K₄Fe(CN)₆/K₃Fe(CN)₆ in 0.1 M PBS buffer solution (pH 7.0) under ambient conditions.

To determine the optimum concentration of DNA probe to be deposited onto the DEP chip surface in order to achieve maximum surface coverage and to reduce the effect of non-specific binding subsequently, probe optimization experiments were performed using electrochemical impedance spectroscopy (EIS) which is widely known to be highly sensitive for such task.²⁶⁻²⁸

A series of DNA probe concentrations were employed for the optimization study and their impedimetric responses were recorded and represented as histograms in Figure 2. As depicted in Figure 2, it can be observed that the intensity of impedimetric signal increases from 0.001 μM to 10 μM before experiencing a slight decrease at 20 μM. The impedimetric signal arises from the charge transfer resistance between the Fe(CN)₆^{3-/4-} redox probe and the DEP chip surface. With the immobilization of DNA probe onto the surface of the DEP chip, enhancement of the charge transfer resistance is expected. This is because DNA probe contains negatively charged phosphate backbone which will in turn lead to repulsion with the similarly negatively charged redox probe and further hinder charge transfer, resulting in the charge transfer resistance to increase and thus a larger impedimetric signal. Therefore, with increasing concentration of DNA probe being immobilized onto the DEP chip surface, there will be greater repulsion of the redox probe and the magnitude of impedimetric signal will increase. As such, at 10 μM of DNA probe which produced the greatest impedimetric signal, it has the highest amount of DNA probe immobilized on the DEP chip surface and thereby capable of providing the maximum coverage of DEP chip surface. Hence, the optimum concentration of DNA probe to be deposited onto the DEP chip surface was established to be 10 μM.

Since the voltammetric signal stemming from the oxidation of MoS₂ nanoflakes was utilized as the analytical signal in this report, it is hence crucial to determine the proper concentration of MoS₂ nanoflakes to be employed for final labelling step.

To do so, a calibration with various concentrations of MoS₂ nanoflakes, obtained by serial dilution from the stock solution, was carried out. The histograms illustrated in Figure 3 represent the voltammetric peak height of MoS₂ nanoflakes oxidation in relation to the different concentrations of MoS₂ nanoflakes. For each individual concentration, DNA hybridization was performed with the complementary (yellow), single-base mismatch (light blue) and non-complementary (pink) sequences. From Figure 3, it is noticed that the voltammetric peak height is the greatest at 0.018 mg/mL. In addition, at 0.018 mg/mL, there is also maximum discrimination among the three different sequences. Henceforth, this concentration of MoS₂ nanoflakes was used for subsequent experimental studies.

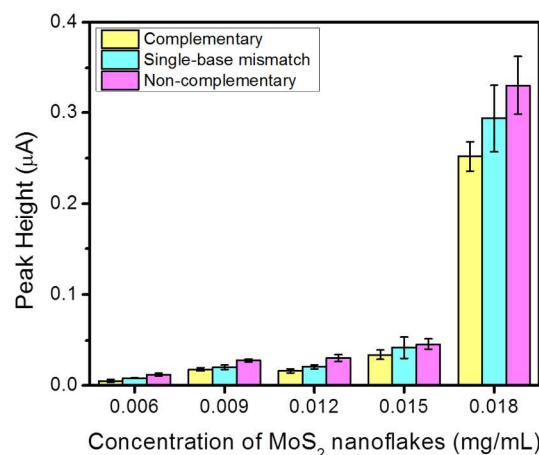


Figure 3. Histograms representing the voltammetric response towards different concentration of MoS₂ nanoflakes employed. Error bars correspond to the standard deviations obtained from triplicate experiments. The concentration of DNA probe and DNA targets used was 10 μM and 300 nM respectively. All electrochemical measurements were conducted in 0.1 M PBS buffer solution (pH 7.0) under ambient conditions.

The voltammetric response of the proposed biosensor towards various concentrations of the complementary DNA sequence was next assessed with the aim of defining the range of detection. As displayed in Figure 4, the voltammetric peak height decreases with increasing concentration of complementary DNA sequence for the range of 0.03 nM to 300 nM with good linearity. Furthermore, it should also be highlighted that the percentage relative standard deviation (% RSD) values exhibited for the calibration plot are lower than 10 %, suggesting good reproducibility. Therefore, the range of detection was determined to be from 0.03 nM to 300 nM, which is of four orders of magnitude.

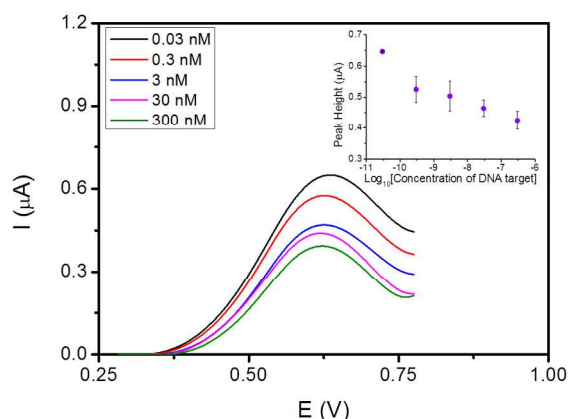


Figure 4. Differential pulse voltammograms of MoS₂ nanoflakes oxidation peak when DNA hybridization was conducted with 0.03 (black), 0.3 (red), 3 (blue), 30 (pink) and 300 (green) nM of complementary DNA sequence. The inset demonstrates the calibration curve of the voltammetric response to the concentration of complementary DNA sequence. Error bars correspond to the standard deviations obtained from triplicate experiments. The concentration of DNA probe and MoS₂ nanoflakes utilized was 10 μM and 0.018 mg/mL respectively. All electrochemical measurements were conducted in 0.1 M PBS buffer solution (pH 7.0) under ambient conditions.

Conclusion

In summary, we have shown that the differential affinity of molybdenum disulfide nanoflakes towards single-stranded DNA and double-stranded DNA, coupled with its electrochemical behavior, can be exploited for the detection of DNA hybridization, correlating to the diagnosis of Alzheimer's disease, with the nanoflakes playing the role of an electroactive label. The electrochemical behavior of molybdenum disulfide nanoflakes, specifically the oxidation peak, was utilized as the analytical signal in the proposed biosensing assay. Based on the proposed biosensing assay, the optimum concentration of DNA probe to be

immobilized onto the disposable electrical printed chip surface was determined to be 10 μM while the optimum concentration of molybdenum disulfide nanoflakes to be employed as electroactive labels was verified to be 0.018 mg/mL. In addition, the range of detection was established to be from 0.03 nM to 300 nM, which is of four orders of magnitude.

A novel approach for the utilization of molybdenum disulfide in the field of biosensing was demonstrated in this study, whereby molybdenum disulfide nanoflakes were employed as electroactive labels. The use of transition metal dichalcogenides such as molybdenum disulfide for sensing and biosensing purposes is a recent research field which holds great potential. Hence, the findings presented in this report are expected to have an immense influence on future work.

Experimental Section

Materials

Molybdenum disulfide (MoS₂) nanoflakes solution was purchased from Graphene Laboratories Inc. (Calverton, New York), with lateral size ranging from 100 to 400 nm and thickness of 1 to 8 layers.

Hydrochloric acid (HCl) (conc. 37%), sodium phosphate dibasic salt (Na₂HPO₄), sodium chloride (NaCl), potassium hexacyanoferrate (II) trihydrate (K₄Fe(CN)₆·3H₂O), potassium hexacyanoferrate (III) (K₃Fe(CN)₆) and DNA oligonucleotides were purchased from Sigma-Aldrich (Singapore). The DNA sequences are as follows:

DNA probe: 5'-ACC AGG CGG CCG CAC ACG TCC TCC AT-3'

Complementary target: 5'-ATG GAG GAC GTG TGC GGC CGC CTG GT-3'

Single-base mismatch target: 5'-ATG GAG GAC GTG CGC GGC CGC CTG GT-3'

Non-complementary target: 5'-AAA AAA AAA AAA AAA AAA AAA AAA AA-3'

Trisodium citrate dihydrate (Na₃C₆H₅O₇·2H₂O) was purchased from Alfa Aesar (Singapore).

Ultrapure water used in this study was obtained from a Milli-Q ion exchange column (Millipore) of resistivity of 18.2 MΩ cm.

The following buffers were used in this study:

0.1 M PBS (0.1 M NaCl + 10 mM Na₂HPO₄, pH 7.0)

TSC 1 (0.75 M NaCl + 75 mM trisodium citrate, pH 7.0)

TSC 2 (0.30 M NaCl + 30 mM trisodium citrate, pH 7.0)

Disposable electrical printed (DEP) carbon chips were obtained from BioDevice Technology (Nomi, Japan). A three-electrode system was employed in this study which included a carbon-based working and counter electrode, and a Ag/AgCl reference electrode.

Equipment

All electrochemical measurements were performed with a μ Autolab type III electrochemical analyzer (Eco Chemie, Utrecht, The Netherlands) connected to a personal computer.

Differential pulse voltammetry (DPV) measurements were controlled by General Purpose Electrochemical System (GPES) software version 4.9 and the parameters applied were: 50 ms modulation time, 0.5 s interval time, 10 mV step potential, 50 mV modulation amplitude and 20 mV/s scan rate. DPV measurements were conducted in 0.1 M PBS buffer solution (pH 7.0) and the raw data produced were treated with a baseline correction of peak width 0.01 using the GPES software.

Impedance measurements were controlled by NOVA software version 1.9 and recorded between 0.1 MHz and 0.1 Hz at a sinusoidal voltage perturbation of 10 mV amplitude. The measurements were performed with 10 mM $K_4Fe(CN)_6/K_3Fe(CN)_6$ (1:1 molar ratio) in 0.1 M PBS buffer solution (pH 7.0) as the redox probe. Randles equivalent circuit was used to fit the obtained impedance spectra, represented as Nyquist plots in the complex plane.

All electrochemical measurements were conducted under ambient conditions by utilizing DEP carbon chips unless otherwise stated.

Procedures

DNA probe was immobilized on the surface of DEP carbon chip by dry physical adsorption. A 3 μ L aliquot of DNA probe solution in PBS buffer at the optimum concentration of 10 μ M was deposited onto the DEP chip surface and left in the oven for 10 minutes at 60 $^{\circ}$ C for drying. After which, the DNA probe modified DEP chip was washed twice in PBS buffer solution with gentle stirring at 25 $^{\circ}$ C in order to remove the excess DNA probe which was not well adsorbed.

The DNA probe modified DEP chip then underwent incubation with hybridization solution (TSC 1 buffer) containing desired concentrations of DNA targets, with the total volume fixed at 100 μ L. The incubation step was performed at 42 $^{\circ}$ C for 30 minutes with gentle stirring. Subsequently, two washing steps were conducted in TSC 2 buffer.

Conjugation with MoS_2 nanoflakes was next carried out by incubating the modified DEP chip with 100 μ L of MoS_2 nanoflakes solution at the desired concentration in PBS buffer. The incubation was performed for 20 minutes at 25 $^{\circ}$ C with gentle stirring. After which, two washing steps in PBS buffer was conducted.

Acknowledgements

M. P. acknowledges Tier 2 grant (MOE2013-T2-1-056; ARC 35/13) from Ministry of Education, Singapore.

Notes

Division of Chemistry & Biological Chemistry, School of Physical and Mathematical Sciences, Nanyang Technological University

21 Nanyang Link, Singapore 637371, Singapore.

Fax: (+) (65) 6791 1961

E-mail: a.bonanni@ntu.edu.sg; pumera@ntu.edu.sg;

pumera.research@outlook.com

References

1. a) M. Chhowalla, H. S. Shin, G. Eda, L. J. Li, K. P. Loh and H. Zhang, *Nature Chem.*, 2013, **5**, 263-275. b) M.

- Pumera, Z. Sofer, A. Ambrosi, J. Mater. Chem. A, 2014, **2**, 8981-8987. c) M. Pumera, A. H. Loo, Trends Anal. Chem, 2014, doi: 10.1016/j.trac.2014.05.009
2. Z. Zeng, Z. Yin, X. Huang, H. Li, Q. He, G. Lu, F. Boey and H. Zhang, *Angewandte Chemie International Edition*, 2011, **50**, 11093-11097.
3. K. G. Zhou, N. N. Mao, H. X. Wang, Y. Peng and H. L. Zhang, *Angew Chem Int Edit*, 2011, **50**, 10839-10842.
4. K. F. Mak, K. L. He, J. Shan and T. F. Heinz, *Nat. Nanotechnol.*, 2012, **7**, 494-498.
5. H. L. Zeng, J. F. Dai, W. Yao, D. Xiao and X. D. Cui, *Nat. Nanotechnol.*, 2012, **7**, 490-493.
6. T. Cao, G. Wang, W. P. Han, H. Q. Ye, C. R. Zhu, J. R. Shi, Q. Niu, P. H. Tan, E. Wang, B. L. Liu and J. Feng, *Nat Commun*, 2012, **3**.
7. K. J. Huang, L. Wang, Y. J. Liu, H. B. Wang, Y. M. Liu and L. L. Wang, *Electrochim. Acta*, 2013, **109**, 587-594.
8. G. Eda, H. Yamaguchi, D. Voiry, T. Fujita, M. W. Chen and M. Chhowalla, *Nano Lett.*, 2011, **11**, 5111-5116.
9. A. Splendiani, L. Sun, Y. B. Zhang, T. S. Li, J. Kim, C. Y. Chim, G. Galli and F. Wang, *Nano Lett.*, 2010, **10**, 1271-1275.
10. Z. Y. Yin, H. Li, H. Li, L. Jiang, Y. M. Shi, Y. H. Sun, G. Lu, Q. Zhang, X. D. Chen and H. Zhang, *ACS Nano*, 2012, **6**, 74-80.
11. S. Bertolazzi, J. Brivio and A. Kis, *ACS Nano*, 2011, **5**, 9703-9709.
12. B. Radisavljevic, A. Radenovic, J. Brivio, V. Giacometti and A. Kis, *Nat. Nanotechnol.*, 2011, **6**, 147-150.
13. G. F. Ma, H. Peng, J. J. Mu, H. H. Huang, X. Z. Zhou and Z. Q. Lei, *J. Power Sources*, 2013, **229**, 72-78.
14. X. Zhong, H. D. Yang, S. J. Guo, S. W. Li, G. L. Gou, Z. Y. Niu, Z. P. Dong, Y. J. Lei, J. Jin, R. Li and J. T. Ma, *J. Mater. Chem.*, 2012, **22**, 13925-13927.
15. K. J. Huang, Y. J. Liu, H. B. Wang, Y. Y. Wang and Y. M. Liu, *Biosens. Bioelectron.*, 2014, **55**, 195-202.
16. H. Li, Z. Y. Yin, Q. Y. He, H. Li, X. Huang, G. Lu, D. W. H. Fam, A. I. Y. Tok, Q. Zhang and H. Zhang, *Small*, 2012, **8**, 63-67.
17. S. X. Wu, Z. Y. Zeng, Q. Y. He, Z. J. Wang, S. J. Wang, Y. P. Du, Z. Y. Yin, X. P. Sun, W. Chen and H. Zhang, *Small*, 2012, **8**, 2264-2270.
18. Y. J. Zhang, J. T. Ye, Y. Matsuhashi and Y. Iwasa, *Nano Lett.*, 2012, **12**, 1136-1140.
19. C. F. Zeng, H. Li, F. Li, C. H. Fan and H. Zhang, *J. Am. Chem. Soc.*, 2013, **135**, 5998-6001.
20. J. Ge, E. C. Ou, R. Q. Yu and X. Chu, *Journal of Materials Chemistry B*, 2014, **2**, 625-628.
21. T. Y. Wang, H. C. Zhu, J. Q. Zhuo, Z. W. Zhu, P. Papakonstantinou, G. Lubarsky, J. Lin and M. X. Li, *Anal. Chem.*, 2013, **85**, 10289-10295.
22. S. Su, H. F. Sun, F. Xu, L. H. Yuwen and L. H. Wang, *Electroanalysis*, 2013, **25**, 2523-2529.
23. J. W. Huang, Z. P. Dong, Y. R. Li, J. Li, W. J. Tang, H. D. Yang, J. Wang, Y. Bao, J. Jin and R. Li, *Mater. Res. Bull.*, 2013, **48**, 4544-4547.

-
24. Q. Feng, K. Duan, X. Ye, D. Lu, Y. Du and C. Wang, *Sensors and Actuators B: Chemical*, 2014, **192**, 1-8.
25. K. J. Huang, J. Z. Zhang, Y. J. Liu and L. L. Wang, *Sensor Actuat B-Chem*, 2014, **194**, 303-310.
- 5 26. M. E. Orazem, and B. Tribollet, *Electrochemical Impedance Spectroscopy*, Wiley-Interscience, Hoboken, New Jersey, 2008.
27. A. Bonanni, M. Pumera and Y. Miyahara, *Anal. Chem.*, 2010, **82**, 3772-3779.
- 10 28. A. Bonanni, M. J. Esplandiu, M. I. Pividori, S. Alegret and M. del Valle, *Anal. Bioanal. Chem.*, 2006, **385**, 1195-1201.